*Structural Chemistry, Vol. 16, No. 6, December 2005 (© 2005)*
DOI: 10.1007/s11224-005-6097-2

# Non-Bonded Intermolecular Interactions and Crystal Stability of *trans*-1,4-Cyclohexanedicarboxylic Acid, 1,4-dibromo

**Gustavo Echeverría,[1,2,3] Adolfo Fantoni,[1] Julio Marañón,[1] and Graciela Punte[1]**

*Received February 24, 2005; accepted May 24, 2005*

Molecular geometry, crystal packing and thermal stability of *trans*-1,4-cyclohexanedicarboxylic acid, 1,4-dibromo (**I**) are examined, in order to analyse the relative influence of the different intermolecular interactions at play. From a comparison with the corresponding properties of *trans*-1,4-cyclohexanedicarboxylic acid (**II**), some insights on the results of the competition between Br and carboxylic groups are obtained. In the crystalline state, the molecules of both compounds present chair centrosymmetric geometry and build infinite chains through ring hydrogen bonds involving the carboxylic groups. These groups are axial in **I** and equatorial in **II**, giving rise to different assembly of the chains. In both compounds there is in general good agreement between the in-crystal geometry and the B3LYP/LanL2DZ optimized geometry of the corresponding isolated molecule. The only significant differences are related to the carboxylic groups. The intermolecular contacts in **I** have been rationalized on the basis of a graph set analysis. A molecular dynamics based method has been used to analyse the temperature dependence of the mean life time of the different kinds of hydrogen bonds characterized in **I**. It has been found that the $O—H\cdots O$ and $C—H\cdots O$(carbonyl) interactions are the main source of thermal stability. The melting point of **I** determined within this approach agrees very well with the experimental value.

**KEY WORDS:** Crystal packing; molecular dynamics; thermal stability; hydrogen bond.

## INTRODUCTION

The knowledge of the influence of different substituents on the supramolecular association of a given fragment and its consequences on the thermal stability of the resulting structures is crucial for designing materials with specific properties.

In a previous study of the crystal polarity and thermal stability of *trans*-l,4-di- and tetra-symmetrically substituted cyclohexanes, we have investigated the influence of different substituents on crystal packing and thermal stability. Symmetric substitution of cyclohexane with C(O)OCH$_3$ [1], CN [2], Br [3], C(O)OH [4] or C(O)NH$_2$ [1] produce crystals whose molecules are in a chair conformation with the substituents equatorial. With the only exception of the dicarboxamide, the resulting crystals are centrosymmetric. It is worth noting that melting points of all these substituted compounds are higher than that of the parent [5].

In the above-mentioned study, the effect of simultaneous substitution with Br and a second substituent in 1 and 4 positions was also analysed (see Scheme 1).

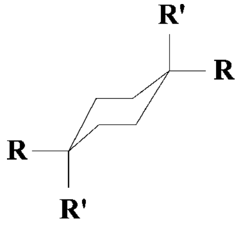

|  | R | R' |
|---|---|---|
| I | C(O)OH | Br |
| II | C(O)OH | H |
| III | Br | C(O)OCH$_3$ |
| IV | CN | Br |
| V | C(O)NH$_2$ | Br |

**Scheme 1.** Chemical diagrams of compounds **I–V**.

---

[1] IFLP. Depto. de Física, Facultad de Ciencias Exactas, Universidad Nacional de La Plata, C.C.67(1900) La Plata, Argentina.

[2] Facultad de Ingeniería, Universidad Nacional de La Plata, C.C.67(1900) La Plata, Argentina.

[3] To whom all corespondence should be addressed at IFLP. Depto. de Física, Facultad de Ciencias Exactas, UNLP, C.C.67(1900) La Plata, Argentina; e-mail: geche@fisica.unlp.edu.ar.

In the molecules of *trans*-1,4-cyclohexanedicarboxylic acid, 1,4-dibromo, dimethyl ester (**III**), Br atoms substitute the axial hydrogens [6]. In contrast in *trans*-1,4-cyclohexanedicarbonitrile, 1,4-dibromo (**IV**) and *trans*-1,4-cyclohexanedicarboxylic acid, 1,4-dibromo (**I**) molecules the Br forces the other substituent to the axial position [7, 8]. Unfortunately, the crystal structure of the *trans*-1,4-cyclohexanedicarboxamide, 1,4-dibromo (**V**) could not be determined.

Melting points of **III** and **IV** are higher than those of the corresponding compounds without Br, while the inverse is true for **V** [9]. As regards the title compound (**I**), its melting point is very similar to that of the *trans*-1,4-cyclohexanedicarboxylic acid (**II**) [9]. Thus, it appears that significant increments in melting points upon Br inclusion are observed when the other substituent does not have a strong hydrogen bond (HB) formation capability, independently of its size and axial or equatorial position.

All these features led us to consider these systems as very good candidates to perform detailed analyses of the intermolecular interactions as a function of the temperature, based on molecular dynamics (MD) simulations. We were in fact aware that several contributions to the understanding of the thermal stability of molecular crystals—mainly through the analysis of the melting process—have been made in the past using methods based on MD simulations [10–12]. In particular, Caffarena *et al.* successfully used a method based on the mean life time of intermolecular hydrogen bonds to determine the melting point of the $\beta$-D-glucose crystals and to study the formation of a glassy state from the fluid [12]. In view of the conclusions drawn by Steiner [13] in their recent work on the competition between different hydrogen bond acceptors for the strong carboxyl donor, we decided to adapt the Caffarena *et al.* method to get insight into the role of the different intermolecular interactions in the thermal stability of substituted cyclohexanes.

Due to its orthorhombic crystal symmetry, compound **I** was considered the most suitable for a first implementation of the method.

In order to obtain a detailed characterisation of the interactions at play, a graph set analysis [14] has been performed.

Some hints on the intermolecular interactions in **I** and **II** have also been searched for from a comparison of the in-crystal geometries with their *ab initio* optimized counterparts.

All the obtained results are presented here.

## CALCULATIONS

### *Ab Initio*

Molecular orbital calculations were performed using the GAUSSIAN 98 program [15]. Geometry optimisations were done at the B3LYP/LanL2DZ level, applying standard gradient techniques. Default convergence criteria were used for SCF and geometry optimisation. The crystallographic geometry [7] was used as the starting point. Centrosymmetric constraints were employed.

### Molecular Dynamics

MD simulations were carried out using the GROMOS 87 package [16]. The Gromos 37C4 force field was used, with the only exception of the atomic partial charges. These were derived, for the experimental molecular geometry, from a fitting of the electrostatic potential within the MKS scheme at the HF/LanL2DZ level. No special potentials were used to simulate hydrogen bonds. In the Gromos force field, L-J coefficients for the 1-4 interactions have special values, in order to avoid any possible excess of repulsive contributions between third neighbours. Since in the crystal the situation usually found between third-neighbours within molecules can also be found between atoms belonging to different molecules, the 1-4 L-J coefficients were used for all atoms. No torsional potentials were included to avoid the introduction of a bias in the calculated conformations [17].

Forty-eight molecules (12 unit cells) were placed in a rectangular box of (21.268 × 25.167 × 22.676) Å, using the single crystal X-ray structure determined at 150 K as the starting point. An integration step of 2 fs was used. Periodical boundary conditions were applied. The cut off radio was set at 10.5 Å. SHAKE was used to constrain all bond lengths to their initial values (tolerance 0.0001 Å).

In order to perform simulations at different temperatures, weak coupling of the system to thermal baths was used, with a relaxation time of 0.02 ps. The system was also coupled to an atmospheric pressure bath with a relaxation time of 0.5 ps.

## RESULTS AND DISCUSSION

### Crystal Packing Analysis

The $\alpha,\beta$-saturated carboxylic acid adopts, in general, the $C^{\alpha}—C^{\beta}—C{=}O$ synplanar conformation [18], as in **I**

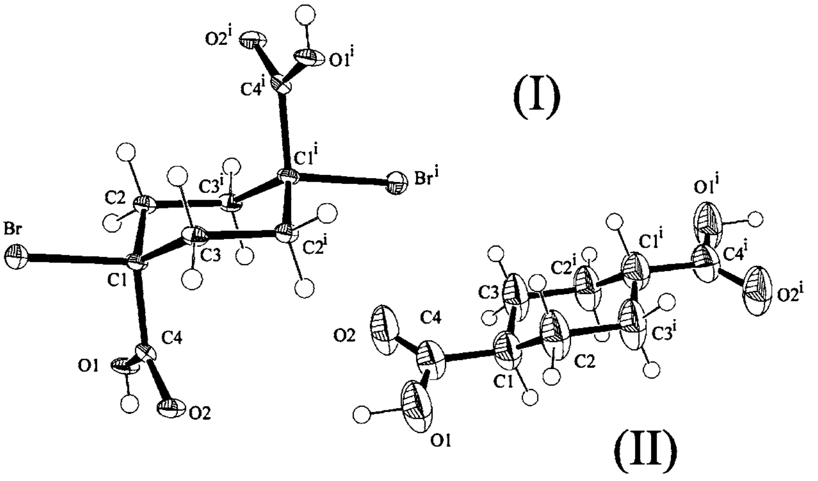

**Fig. 1.** Fifty percent probability ORTEP [19] drawing of the molecules of *trans*-1,4-cyclohexanedicarboxylic acid, 1,4-dibromo (**I**) [7] and *trans*-1,4-cyclohexanedicarboxylic acid (**II**) data from Dunitz *et al.* [4].

and **II** crystals (Fig. 1). In this conformation the carboxylic moiety can form two different HB patterns depending on the residue. They are referred to as catemer (see Scheme 2) and cyclic dimer motifs [18, 20]. The latter is less dependent on the size and shape of the residue and is more usually found in solid state. In dicarboxylic acids with antiparallel carboxylic groups, the molecules form infinite chains of cyclic HB dimers (see Scheme 2), as found in **II** and **I**—in spite of the axial location of the carboxylic group in the later [7]. The graph set analysis [14] of **I** crystal structure, showed that the molecules, located at inversion centres, are linked by $\mathbf{R}_2^2(\mathbf{8})$[4] rings forming infinite chains described at the unitary level as a **C**(**9**)[$\mathbf{R}_2^2(\mathbf{8})$] graph set (Fig. 2a). Each chain, running along *b* axis, is surrounded by four neighbouring chains shifted half a primitive *b* vector length along chain direction. This chain arrangement favours the four carbons of the cyclohexane rings, which are donors in C—H···O interactions, being located near the proton acceptor oxygen atoms of the adjacent chain carboxylic groups, helping interchain HB interactions. These C—H···O interactions connect the **C**(**9**)[$\mathbf{R}_2^2(\mathbf{8})$], forming a HB network (Table I) that stabilize the three-dimensional crystal structure. At the first level, the C—H···O network can be described as infinite **C**(**5**) motifs directed along the three crystallographic axes.

The motif built on interactions involving axial hydrogen atoms ($H_{ax}$) gives rise to infinite chains running along *b*. Those built on interactions involving equatorial hydrogen atoms, instead, form infinite chains running along *a* and along *c*. As can also be seen in Table I, the axial and equatorial hydrogen atoms form HBs with both, hydroxyl and carbonyl oxygen atoms. Higher level motifs are developed in **I** when the various **C**(**5**) and **C**(**9**)[$\mathbf{R}_2^2(\mathbf{8})$] chains are considered. The equatorial bromine atoms are piled up along *b*, this arrangement being similar to that observed in other 1,4-Br substituted cyclohexane derivatives whose melting points (m.p.) increase upon Br inclusion. Br···Br distance in **I** (4.1919(5) Å), however, is larger than in the other derivatives. Although the importance of the Br···Br

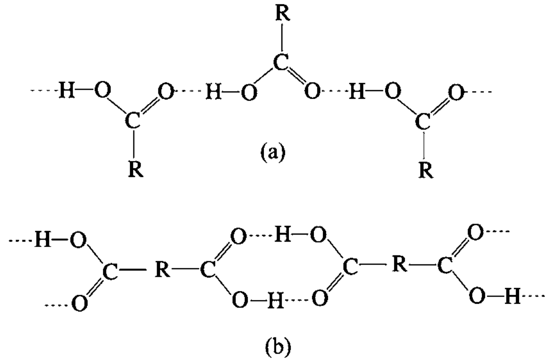

**Scheme 2.** Carboxylic group HB patterns: (a) cyclic dimer and (b) catemer.

---

[4] According to Bernstein *et al.* [14(b)] graph sets are denoted by $G_d^a(n)$ where G stands for the pattern designator (C: chain; R: ring; etc.); *d* and *a* describe the number of donors and acceptors, respectively; and *n* is the number of atoms involved.

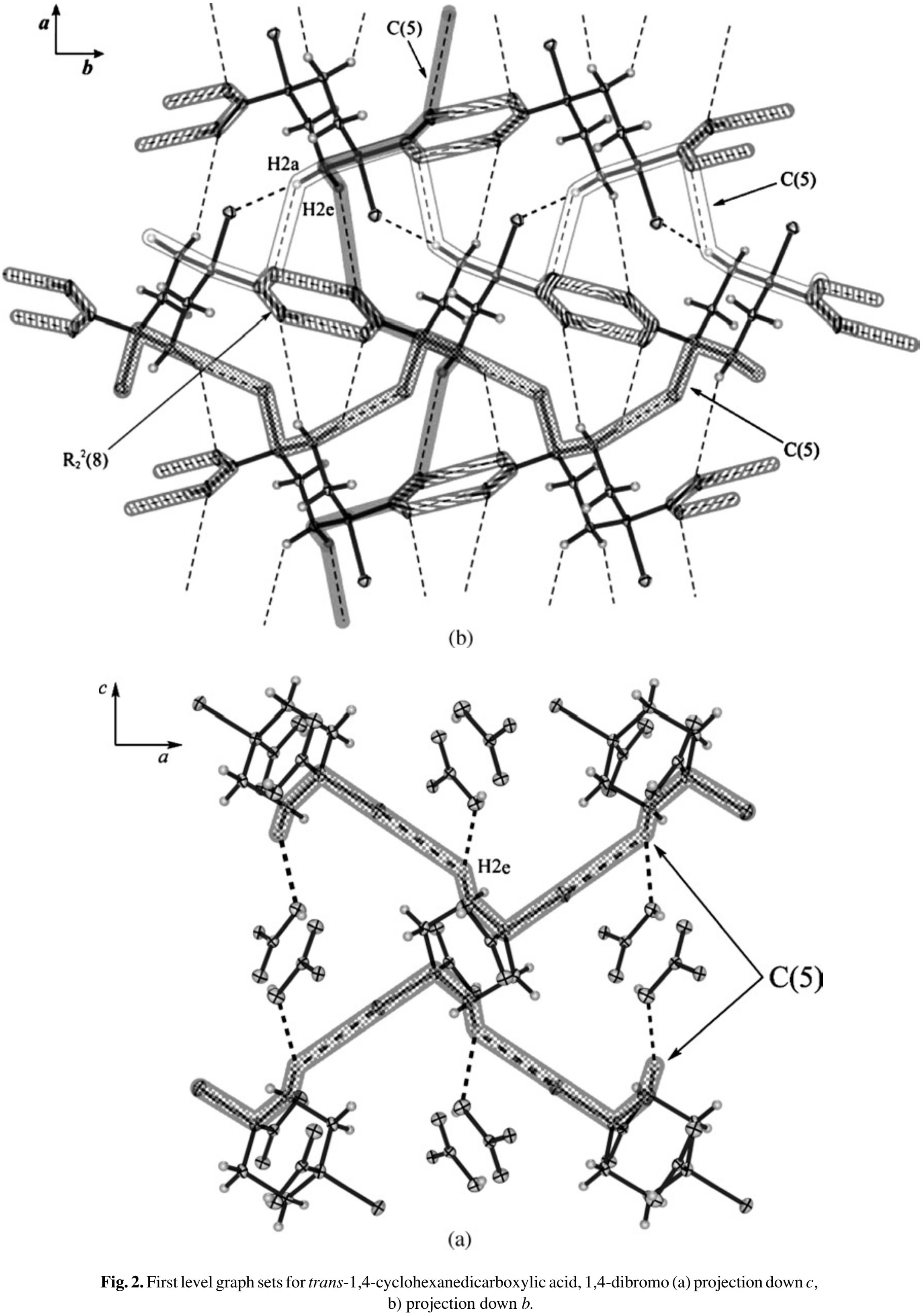

**Fig. 2.** First level graph sets for *trans*-1,4-cyclohexanedicarboxylic acid, 1,4-dibromo (a) projection down *c*, b) projection down *b.*

**Table I.** Observed Hydrogen Bond Geometry of **I** and **II**

| | HB | D—H[a] | H···A[a] | D—H···A[a] | H···A—X[a] | $N_1$[b] |
|---|---|---|---|---|---|---|
| **I** | O—H···O(sp$^2$) | 0.82 | 1.8202 | 176.3 | 123.3 | $\mathbf{R_2^2(8)}$ |
| | C2—H2a···O(sp$^3$) | 0.97(3) | 2.73(2) | 116(2) | 146.0(7) | C(5) |
| | C2—H2e···O(sp$^2$) | 0.96(2) | 2.93(2) | 140(2) | 147.9(1) | C(5) |
| | C3—H3a···O(sp$^2$) | 1.01(3) | 2.71(3) | 129(2) | 107.5(5) | C(5) |
| | C3—H3e···O(sp$^3$) | 0.96(3) | 3.18(3) | 132(2) | 129.4(6) | C(5) |
| | C2—H2a···Br | 0.96(3) | 3.17(3) | 157.1(2) | 134.7(5) | C(4) |
| | C2—H2e···Br | 0.96(2) | 3.03(2) | 139.0(2) | 159.9(5) | C(4) |
| **II** | O—H···O(sp$^2$) | 0.9953 | 2.7900 | 138.75 | 104.46 | $\mathbf{R_2^2(8)}$ |
| | Cl—Hl···O(sp$^3$) | >1.1035 | 2.8222 | 126.11 | 132.88 | C(4) |
| | C2—H2a···O(sp$^2$) | >1.0919 | 2.5401 | 160.61 | 136.39 | C(5) |
| | C2—H2e···$\pi$(C═O) | 1.0234 | 2.9581 | 156.82 | 83.38 | C(5) |
| | C3—H3a···O(sp$^3$) | 0.9917 | 2.7990 | 159.19 | 115.06 | C(5) |
| | C3—H3e···$\pi$(C═O) | >1.0922 | 2.9383 | 141.84 | 78.99 | C(5) |

[a] D and A are proton donor and acceptor atoms, respectively, and X: C4 or C1.

[b] $N_1$ correspond to the first level motif, containing one type of hydrogen bond [14].

interactions in the molecular recognition process and in the stability of organic crystals has been claimed by different authors [21], it is still a matter of controversy. In particular, Dance [22] questions the use of geometrical criteria to verify the existence of attractive forces. From our results, some connection between the lack of m.p. increment in going from **II** to **I** and the large value of the Br···Br distance in the later can in principle be inferred.

The above-described Br arrangement is surrounded by four $\mathbf{C(9)[R_2^2(8)]}$, favouring the formation of C—H···Br interactions, in which only one of the non-equivalent ring C atoms participates, but instead with its two hydrogen atoms (see Table I). At first level, both HB interactions can be described as infinite chains of **C(4)** type. The chains built on C—$H_{ax}$···Br interactions, lying on the (0 0 1) plane, are directed along the *b* axis, whereas those built on C—$H_{eq}$···Br interactions, lying on the (0 1 0) plane, are directed along axis *a* (Fig. 2b).

Crystal packing of **II** can also be described as consisting of chains of $\mathbf{C(9)[R_2^2(8)]}$, along the *c* axis, connected with other six neighbouring chains by C—H···O interactions. The H atoms bound to the four ring unsubstituted carbons, as found in **I**, form C—$H_{ax}$···O and C—$H_{eq}$···O interchain interactions of **C(5)** type. On the other hand, the H bound to the ring substituted carbon atoms form a C—$H_{ax}$···O interchain interaction of **C(4)** type (Fig. 3 and Table I).

The interaction between carboxylic acid dimers has been studied by Leizerowitzs. Based on coulombic interactions he was able to explain the formation of the four distinctive stacking patterns of $\mathbf{R_2^2(8)}$ motifs. In **II** packing analysis allows to identify a distorted version of one of the four stacking patterns of cyclic dimers of carboxylic acids depicted by Leiserowitz [18]. None of those stacking patterns could be recognized in **I**.

## *Ab Initio* Results

Some hints on the influence of the crystal environment on the molecular structure can be obtained from a comparison between the free molecule and in-crystal molecular geometries. The most relevant experimental and calculated bond length and angles can be seen in Table II. In both compounds the most important discrepancies between experimental and calculated bond lengths and angles correspond to the carboxylic moiety, involved in the strong ring hydrogen bonds described above. The shortening of the C—OH bond length in the crystals can be associated with the inherent proton tunnelling that would also be present at low temperature [23].

Some interesting features of **I** molecules, instead, would in principle not be due to packing effects, since they are observed in both the experimental and calculated data: (1) Br—C—COOH angle (~102.8°) is smaller than the H—C—H angle in gas phase cyclohexane (106.65°) [24]; (2) C—Br bond length is larger than the C—Br bond length observed in *trans*-1,4-dibromocyclohexane (1.834 Å) [3]; (3) C2—C3$^i$ bond lengths are larger than the mean C—C ring bond length.

Since **II** diffraction data have been collected at room temperature, differences between experimental and calculated bond distances might also be due to thermal effects.

## Molecular Dynamics Results

The Caffarena *et al.* method [12] is based on a statistical analysis of the mean life times of intermolecular hydrogen bonds defined on the basis of a geometrical criterion. Since the Van der Waals cut off definition has been shown to be too restrictive [25], we adopted a somewhat

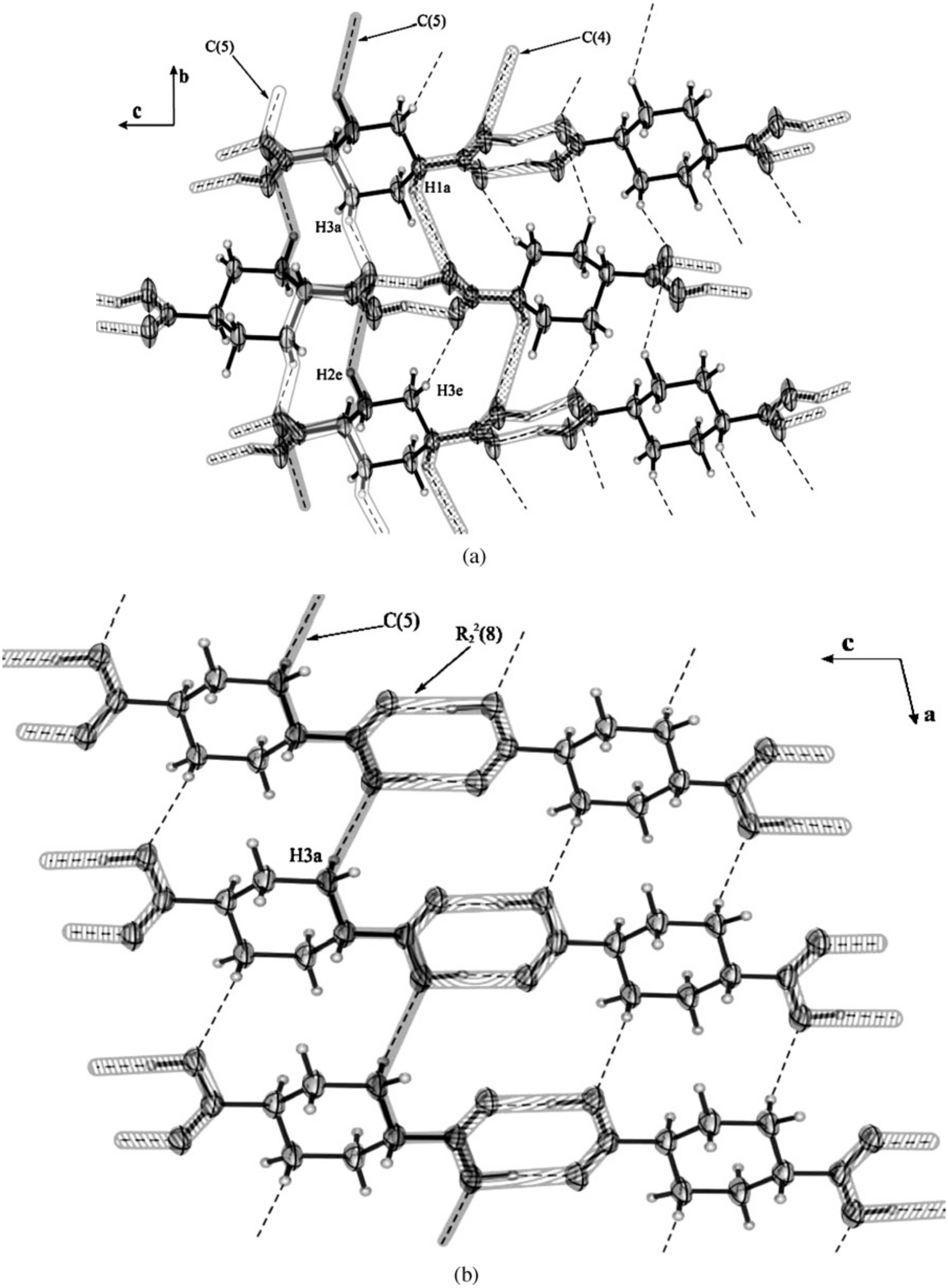

**Fig. 3.** First level graph sets for *trans*-1,4-cyclohexanedicarboxylic acid (a) projection down *b*, (b) projection down *a*.

**Table II.** Calculated (B3LYP/LanL2DZ) and Experimental Selected Molecular Parameters

| | I | | II | |
|---|---|---|---|---|
| | Calculated | Experimental | Calculated | Experimental |
| (a) Bond distances | | | | |
| Cl—X[a] | 2.088772 | 1.988(2) | 1.099837 | >1.1035 |
| C1—C2 | 1.539061 | 1.525(3) | 1.543862 | 1.512(4) |
| C1—C3 | 1.537807 | 1.525(3) | 1.559422 | 1.510(4) |
| C2—C3 | 1.556455 | 1.546(3) | 1.542917 | 1.527(4) |
| C1—C4 | 1.530742 | 1.536(2) | 1.515045 | 1.502(3) |
| C4—O1 | 1.383092 | 1.304(3) | 1.393061 | 1.295(4) |
| Ol—H | 0.984434 | 0.82 | 0.984809 | >0.9953 |
| C4—O2 | 1.239607 | 1.234(3) | 1.240780 | 1.225(3) |
| C2—H2a | 1.095326 | 0.98(3) | 1.098213 | >1.0919 |
| C2—H2e | 1.092281 | 0.96(2) | 1.097725 | 1.0234 |
| C3—H3a | 1.096081 | 1.01(3) | 1.100615 | 0.9917 |
| C3—H3e | 1.093446 | 0.96(3) | 1.096330 | 1.0922 |
| (b) Bond angles | | | | |
| C3—C1—C2 | 112.0719 | 111.7(2) | 111.0548 | 111.8(2) |
| C1—C2—C3 | 110.7333 | 110.6(2) | 111.2238 | 111.7(2) |
| C2—C3—C1 | 110.8498 | 109.9(2) | 110.9675 | 112.3(2) |
| X[a]—Cl—C4 | 102.9963 | 102.2(1) | 107.099 | 113.08 |
| X[a]—Cl—C2 | 107.8999 | 107.7(1) | 109.7824 | 103.63 |
| X[a]—Cl—C3 | 107.782 | 108.9(1) | 107.4278 | 104.43 |
| O1—C4—O2 | 122.02 | 125.0(2) | 121.2512 | 122.1(2) |
| O1—C4—C1 | 112.6728 | 114.4(2) | 111.5625 | 115.0(2) |
| O2—C4—C1 | 125.3047 | 120.6(2) | 127.1777 | 122.9(2) |
| C4—O1—H | 110.8548 | 106(3) | 110.671 | 104.48 |

[a] X: Br or H.

more flexible criterion. An interaction between a donor (D) and an acceptor (A) is considered a hydrogen bond if: (a) the H···A distance is shorter than 3.2 Å ; and (b) the D—H···A angle is larger than 110°. The basic idea is that there is a direct relation between an HB mean life time and its stability, so that the contribution of a specific kind of HB to the crystal stability at a given temperature depends on the corresponding mean life time.

The parameter used in the analysis as a function of the temperature is the average HB total number

$$N_{\mathrm{HB}} = \frac{\sum_i n_i(\tau_i/\tau)}{\sum_i n_i}$$

where $n_i$ is the number of each non-equivalent HBs in the initial ensemble, and $\tau_i$ the corresponding mean life time during a simulation time $\tau$. The summation ranges over the seven non-equivalent HBs that have been identified in **I** and are reported in Table I: the O—H···O described as a $\mathbf{R_2^2(8)}$ motif, the two C—H···Br described as a **C(4)** motif, and the two C—H···O(hydroxyl) and two C—H···O(carbonyl) described as **C(5)** motifs (see Crystal Packing Analysis section and Table I).

After stabilisation at 0 K (90 ps), $N_{\mathrm{HB}}$ has been determined for 24 increasing temperature values (30 ps of stabilisation + 50 ps of data collection). The obtained results are plotted in Fig. 4. As it can be seen, $N_{\mathrm{HB}}$ decreases unevenly as temperature increases. This behaviour is related with the relative stability of the different HBs. At approximately 135 K there is a drop, which can be associated with a rapid reduction in the mean life time of the C—H···Br and C—H···O(hydroxyl) interactions. Above this temperature, the C—H···O(hydroxyl) contributions increase fast, reaching its original value at about 147 K.

The C—H···Br contribution, instead, continues decreasing up to almost zero. This finding can be rationalized taking into account that the involved C—H donors participate in bifurcated interactions, with Br and O(hydroxyl) as acceptors. Therefore, the lessening of C—H···Br interactions would allow a rearrangement of the corresponding C—H donors and O(hydroxyl) acceptors favouring the C—H···O(hydroxyl) interactions. Within the range 147–255 K, the $N_{\mathrm{HB}}$ value remains almost constant. Above 255 K, $N_{\mathrm{HB}}$ decreases slowly. This behaviour corresponds to a reduction of the C—H···O(hydroxyl) contribution, which practically reaches its minimum at about 450 K. At temperatures higher than 450 K the rate of the $N_{\mathrm{HB}}$ reduction is sensibly increased due to a simultaneous

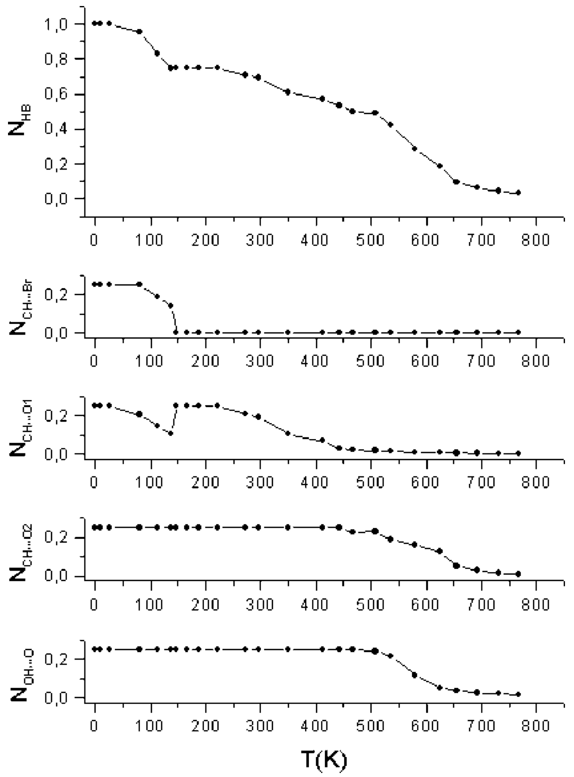

**Fig. 4.** Temperature evolution of the hydrogen bond mean life times. Ol and O2 stand for hydroxyl and carbonyl oxygen atoms, respectively.

diminution of the C—H···O(carbonyl) and the O—H···O interaction contributions. Finally around 655 K, the mean life times of both interactions are almost reaching their minima. The order parameter does not show the sharp drop observed by Caffarena *et al.* for pure glucose [12]. Above 450 K its temperature dependence is instead similar to that observed in the simulations of the melting of pure water [26]. Since the melting point calculated in [26] from a sigmoidal fit is in good agreement with experiment, the same method was applied here (see Fig. 5). The resulting melting point (586(6) K) satisfactorily reproduce the experimental value (577 K) [5].

At this point, some comments on the results obtained by Gavezzotti [11] from a MD study of the melting of acetic acid crystals would be of interest. In that study, it was observed that the strongest intermolecular linkages, the hydrogen bonds, start to break before the weaker collective dispersion interactions are overcome and melting occurs. It was also showed that this behaviour is a consequence of rotational diffusion events which lead to several types of cross-linking among catemer chains through the formation of HBs of different kinds. The resulting rotational defects are easily incorporated into the crystal structure due to the approximate three-fold symmetry of the acetic acid molecule. Because of that, as temperature rises hydrogen bonds become more and more fluxional with relatively little expense of total potential energy, without requiring translational diffusion. As regards the original HBs, the augment in the fluxional behaviour would imply a decrease in their mean life time. Whether the criteria adopted in this paper could also work fine to determine the melting point of acetic acid is difficult to assess, but there is apparently no reason for a negative answer.

Anyway, since in our system rotational diffusion events would hardly be possible before melting, HBs can

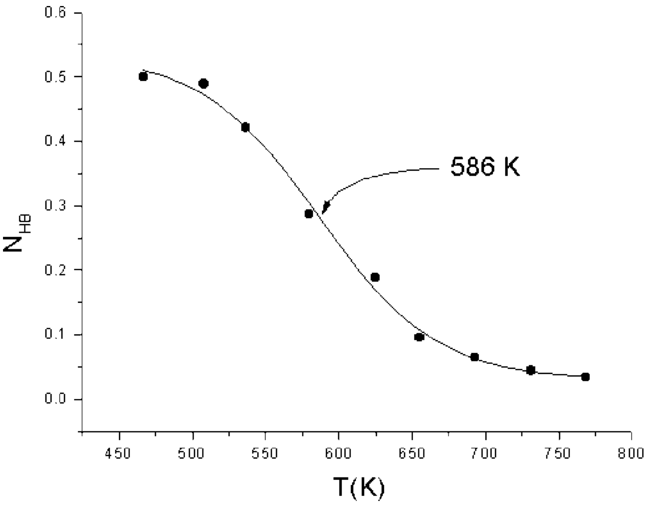

**Fig. 5.** Sigmoidal fit of $N_{\mathrm{HB}}$. The melting point is the abscissa of the inflexion point.

be used with confidence as indicators of crystal stability. That is, though crystal stability is expected to depend on a balanced interplay of different kinds of interactions, if a suitable criterion is adopted in the analysis, very useful information can be obtained from the behaviour of HBs as a function of the temperature.

Finally, it is interesting noting that in spite of the difference in strength, both, the O—H···O and the C—H···O(carbonyl) interactions contribute to crystal stability till melting.

## CONCLUSIONS

A detailed analysis of the intermolecular interactions in *trans*-l,4-dibromo-cyclohexane dicarboxylic acid (**I**) crystal has been performed, also as a function of the temperature. The important conformational effect of Br inclusion, which forces the carboxylic group to the axial position, has almost no influence on the most relevant intermolecular interactions, as can be inferred from the similarity between first level graph set motifs in **I** and **II**. Large Br···Br distances prevent a relevant interaction between Br atoms from being established in **I**. Both results are consistent with the lack of melting point increment in going from **II** to **I**. An adaptation of a quite simple model was applied to evaluate, from molecular dynamics simulation results, the relative influence on crystal stability of different intermolecular hydrogen bond interactions. The obtained results show that at temperatures close to the melting point the O—H···O and C—H···O(carbonyl) are the only HB interactions contributing to crystal stability in **I**.

## ACKNOWLEDGMENTS

Financial support from the Consejo Nacional de Investigaciones Cientificas y Técnicas (CONICET), PIP 0460/98, Facultad de Ciencias Exactas, Universidad Nacional de La Plata, República Argentina, and CSIC, Spain, is greatly acknowledged. A.F., G.E., J.M. and G.P. are members of the CONICET.

## REFERENCES

1. Echeverría, G. *PhD thesis*. Dpto. de Fésica, Fac. de Cs. Exactas, Universidad Nacional de La Plata, Argentina, 1997.
2. Echeverría, G.; Punte, G.; Rivero, E.; Barón, M. *Acta Cryst. C* **1995,** *51*, 1020.
3. Hassel, G.; Hadler Vihovde, E. *Acta Chem. Scand.* **1953,** *7*, 1164.
4. Dunitz, J. D.; Strickler, P. *Helv. Chim. Acta* **1966,** *49*, 2505.
5. Kahn, R.; Fourme, R.; André, D.; Renauld, M. *Acta Cryst. B* **1973,** *29*, 131.
6. Echeverria, G.; Punte, G.; Barón, M. *Struct. Chem.* **2000,** *11*, 35.
7. Echeverría, G.; Goeta, A. E.; Barón, M.; Punte, G. *Acta Cryst. E* **2003,** *59*, o959.
8. Echeverría, G.; Punte, G.; Rivero, E.; Barón, M. *Acta Cryst. C* **1995,** *51*, 1023.
9. Barón, M.; de Zenobi, E. L.; Davidson, M. *J. Mol. Struct.* **1975,** *124*, 432.
10. (a) Allen, M. P.; Tildesley, D. J. *Computer Simulations of Liquids*; Clarendom Press: Oxford, 1987, and references therein; (b) Straub, G. K.; Aidun, J. B.; Wils, J. M.; Sanches-Castro, C. R.; Wallace, D. C. *Phys. Rev. B* **1994,** *50*, 5055; (c) Van Buren, R.; De Vlieg, J.; Berendsen, J. C. *Langmuir* **1995,** *11*, 2957.
11. Gavezzotti, A. G. *J. Mol. Struct.* **1999,** *486*, 488.
12. Caffarena, E.; Grigera, J. R. *J. Chem. Soc. Faraday Trans.* **1996,** *92*, 2285.
13. Steiner, T. *Acta Cryst. B* **2001,** *57*, 103.
14. (a) Bernstein, J.; Davis, R. E. In *Implications of Molecular and Materials Structure for New Technologies*; Howard, J. A. K.; Allen, F. H.; Shields, G. P., Eds.; Kluwer Academic Publishers: The Netherlands, 1999, 275. (b) Bernstein, J.; Davis, R. E.; Shimoni, L.; Chang, N. *Angew. Chem. Int. Ed. Engl.* **1995,** *34*, 1555.
15. Frisch, M. J.; Trucks, G. W.; Schlegel, H. B.; Gill, P. M. W.; Johnson, B. G.; Robb, M. A.; Cheeseman, J. R.; Keith, T.; Petersson, G. A.; Montgomery, J. A.; Raghavachari, K.; Al-Laham, M. A.; Zakrzewski, V. G.; Ortiz, J. V.; Foresman, J. B.; Peng, C. Y.; Ayala, P. Y.; Chen, W.; Wong, M. W.; Andres, J. L.; Replogle, E. S.; Gomperts, R.; Martin, R. L.; Fox, D. J.; Binkley, J. S.; Defrees, D. J.; Baker, J.; Stewart, J. P.; Head-Gordon, M.; Gonzalez, C.; Pople, J. A. Gaussian 94, Revision B.3 Gaussian, Inc.: Pittsburgh, PA, 1995.
16. Van Gunsteren, W. F.; Berendsen, H. J. C. *GROningen Molecular Simulations Package*; BIOMOS, Groningen: The Netherlands, 1987.
17. Franks, F.; Grigera, J. R. *Water Sci. Rev.* **1990,** *5*, 187.
18. Leiserowitz, L. *Acta Cryst. B* **1976,** *32*, 775.
19. Burnett, M. N.; Johnson, C. K. *ORTEP-III. Report ORNL-6895*; Oak Ridge National Laboratory: Oak Ridge, Tennessee, US, 1996.
20. Berstein, J.; Etter, M. C.; Leiserowitz, L. In *Structure Correlation*; Bürgi, H. B.; Dunitz, J. D., Eds.; **1994,** *2*, 431, and references therein.
21. See for example: (a) Desiraju, G. R. *Crystal Engineering*; Elsevier Science Publishers B. V.: Amsterdam, 1989; (b) Echeverría, G.; Punte, G.; Barón, M. *Struct. Chem.* **2000,** *11*, 35; (c) Csóregh, I.; Brehmer, T.; Bombicz, P.; Weber, E. *Cryst. Eng.* **2001,** *4*, 343. These authors appreciation on the influence of C—Br···Br—C interactions in crystal stabilization is upheld even when halogen–halogen distances are larger than the sum of Van der Waals radii, (d) For a recent review see: Metrangolo, P.; Pilat, T.; Resnati, G.; Stevenazzi, A. *Curr. Opin. Colloid Interface Sci.* **2003,** *8*, 215.
22. Dance, I. *New J. Chem.* **2003,** *27*, 22.
23. (a) Meier, B. H.; Graf, F.; Ernst, R. R. *J. Chem Phys.* **1982,** *16*, 767; (b) Nagaoka, S.; Terao, T.; Imashiro, F.; Suika, A.; Hirota, N.; Nayashi, S. *Chem. Phys. Lett.* **1981,** *80*, 580.
24. Dommen, J.; Brupbacher, T.; Grassi, G.; Bauder, A. *J. Am. Chem. Soc.* **1990,** *112*, 953.
25. Steiner, T. *Angew. Chem. Int. Ed.* **2002,** *41*, 48.
26. Caffarena, E.; Grigera, J. R. *Carbohydr. Res.* **1997,** *300*, 51, and references therein.